Nuclear Inst. and Methods in Physics Research, A 940 (2019) 223–229

Contents lists available at ScienceDirect

Nuclear Inst. and Methods in Physics Research, A

journal homepage: www.elsevier.com/locate/nima

Ultrafast inorganic scintillator-based front imager for Gigahertz Hard X-ray imaging

Chen Hu [a], Liyuan Zhang [a], Ren-Yuan Zhu [a,*], Marcel Demarteau [b], Robert Wagner [b], Lei Xia [b], Junqi Xie [b], Xuan Li [c], Zhehui Wang [c], Yanhua Shih [d], Thomas Smith [d]

[a] 256-48, HEP, California Institute of Technology, Pasadena, CA 91125, USA
[b] Argonne National Laboratory, 9700 South Case Avenue, Argonne, IL 60439, USA
[c] Los Alamos National Laboratory, Los Alamos, NM 87545, USA
[d] University of Maryland, Baltimore County, Baltimore, MD 21250, USA

ARTICLE INFO

Keywords:
Ultrafast
Inorganic scintillator
Crystal
Microchannel plate
Rise time
Decay time
FWHM pulse width

ABSTRACT

State-of-the art X-ray imaging cameras using silicon sensors for X-ray detection have demonstrated a frame-rate of 10 MHz and excellent performance for X-ray energies below 20 keV. We proposed a pixelated ultrafast inorganic scintillator-based front imager for GHz hard X-ray imaging. The proposed imager is featured with a total absorption for hard X-ray photons, and provides sub-ns scintillation pulse width crucial for X-ray bunches of a few ns spacing foreseen at the proposed MaRIE facility. We measured temporal response of a dozen ultrafast and fast inorganic scintillators at the 10-ID-B site of the Advanced Photon Source (APS) of ANL. Crystal's response to hybrid X-ray beam of 30 keV, consisting of singlet bunches of 50 ps width and septuplet bunches of 27 ps width with 2.83 ns bunch spacing, was measured. Ultrafast inorganic scintillators, such as BaF_2:Y and ZnO:Ga, show clearly resolved X-ray bunches for septuplets, as well as no degradation of amplitude for continuous eight septuplets, providing a proof of principle for the ultrafast inorganic scintillator-based total absorption front imager for the proposed MaRIE project.

Contents

1. Introduction

Substantial advances have been made in high-speed imaging technologies, including ones for the full spectrum of X-ray wavelengths. Dedicated high-speed imaging technologies have been developed for existing and upcoming X-ray free electron lasers (XFELs) such as LCLS, European XFEL, SACLA, and SwissFEL. Commercial photon-counting cameras such as Pilatus, X-ray integrating detectors or high-speed visible light CCD and CMOS cameras in conjunction with fast scintillators are widely used in many experiments. State-of-the-art X-ray imaging cameras using silicon sensors have demonstrated a frame-rate close to 10 MHz and excellent performance for X-ray imaging at energies below 20 keV.

Aiming at studying the dynamics of material evolution related to the nuclear Big Bang, a Matter-Radiation Interaction in Extreme (MaRIE) facility was proposed by Los Alamos National Lab (LANL) [1], where GHz hard X-ray (> 20 keV) imaging is required. Table 1 lists the technical requirements of hard X-ray imagers for the proposed MaRIE project [2], where 2 ns and 300 ps frame rates are required for the type I and II imager for X-rays up to 30 keV and 126 keV, respectively. To mitigate any pileup effect caused by such fast frame rates it is important to have a temporal response of the X-ray signals of less than 2 ns and 300 ps respectively for the Type I and II imagers. Development of sensors with ultrafast time response for such imager is thus important.

Two types of sensor technologies are being pursued for fast X-ray imaging [2]. The direct sensor technology uses semiconductor devices to convert X-rays to electrons, which are then collected. The indirect sensor technology uses inorganic scintillators to convert X-rays

* Corresponding author.
E-mail address: zhu@hep.caltech.edu (R.-Y. Zhu).

https://doi.org/10.1016/j.nima.2019.06.011
Received 15 November 2018; Received in revised form 27 March 2019; Accepted 7 June 2019
Available online 17 June 2019
0168-9002/

Table 1
Requirements on hard X-ray imagers for the proposed MaRIE project.

Performance	Type I imager	Type II imager
X-ray energy	Up to 30 keV	42–126 keV
Frame-rate/inter-frame time	0.5 GHz/2 ns	3 GHz/300 ps
Number of frames per burst	≥ 10	10–30
X-ray detection efficiency	Above 50%	Above 80%
Pixel size/pitch	≤ 300 μm	<300 μm
Dynamic range	10^3 X-ray Photons/pixel/frame	≥ 10^4 X-ray Photons/pixel/frame
Pixel format	64 × 64[a] (scalable to 1 Mpix)	1 Mpix

[a]In a sense, 64 × 64 is an implementation detail for 1 Mpix camera.

Table 2
Fast and ultrafast crystal scintillators tested for hard X-ray imaging.

	BaF_2	BaF_2 (:Y)	ZnO (:Ga)	YAP (:Yb)	YAG (:Yb)	β -Ga_2O_3	LYSO (:Ce)	LuAG (:Ce)	YAP (:Ce)	GAGG (:Ce)	LuYAP (:Ce)	YSO (:Ce)
Density (g/cm^3)	4.89	4.89	5.67	5.35	4.56	5.94	7.4	6.76	5.35	6.5	7.2[h]	4.44
Melting point (°C)	1280	1280	1975	1870	1940	1725	2050	2060	1870	1850	1930	2070
X_0 (cm)	2.03	2.03	2.51	2.77	3.53	2.51	1.14	1.45	2.77	1.63	1.37	3.10
R_M (cm)	3.1	3.1	2.28	2.4	2.76	2.20	2.07	2.15	2.4	2.20	2.01	2.93
λ_I (cm)	30.7	30.7	22.2	22.4	25.2	20.9	20.9	20.6	22.4	21.5	19.5	27.8
Z_{eff}	51.6	51.6	27.7	31.9	30	28.1	64.8	60.3	31.9	51.8	58.6	33.3
dE/dX (MeV/cm)	6.52	6.52	8.42	8.05	7.01	8.82	9.55	9.22	8.05	8.96	9.82	6.57
λ_{peak}[a] (nm)	300 220	300 220	380	350	350	380	420	520	370	540	385	420
Refractive Index[b]	1.50	1.50	2.1	1.96	1.87	1.97	1.82	1.84	1.96	1.92	1.94	1.78
Normalized Light Yield[a,c,d]	42 4.8	1.7 4.8	6.6[e]	0.19[e]	0.36[e]	6.5 0.5	100	35[g] 48[g]	9 32	115	16 15	80
Total Light yield (ph/MeV)	13,000	2000	2000[e]	57[e]	110[e]	2,100	30,000	25,000[g]	12,000	34,400	10,000	24,000
Decay time[a] (ns)	600 0.6	600 0.6	<1[f]	1.5	4	148 6	40	820 50	191 25	53	1485 36	75
LO in 1st ns (photons/MeV)	1200	1200	610[e]	28[e]	24[e]	43	740	240	391	640	125	318
40 keV Att. Len. (1/e, mm)	0.106	0.106	0.407	0.314	0.439	0.394	0.185	0.251	0.314	0.319	0.214	0.334

[a]Top line: slow component, bottom line: fast component.
[b]At the wavelength of the emission maximum.
[c]Excited by Gamma rays.
[d]Light output of LYSO is defined as 100.
[e]Excited by Alpha particles.
[f]Nanoparticles in polystyrene host [3].
[g]Ceramic with 0.3 g at% co-doping.
[h]Based on $Lu_{0.7}Y_{0.3}AlO_3$:Ce.

to photons that are collected by photodetectors. Both direct and indirect sensors for X-ray detection are currently limited by the materials and their structures. There is a significant gap between the state-of-the art X-ray imaging technologies at about the 10 MHz frame-rate and the performances desired for the proposed MaRIE project. While the direct technology prevails in MHz soft X-ray imaging, it has an intrinsic limitation for GHz hard X-ray imaging because of its low detection efficiency of thin detectors required for fast response. Development of ultrafast inorganic scintillators with a fast rise time, fast decay time and negligible slow scintillation tail is thus crucial for such imagers.

In the past several years, we investigated ultrafast inorganic crystal scintillators for GHz hard X-ray imaging [4,5]. Table 2 lists basic properties for a dozen of fast and ultrafast inorganic scintillators, where their light output is listed in a reference to cerium doped lutetium oxy-orthosilicate (LSO:Ce) and lutetium yttrium oxyorthosilicate (LYSO:Ce) because of their superb performance and wide applications. Among the inorganic scintillators listed in Table 2, only three scintillators, barium fluoride (BaF_2), yttrium doped barium fluoride (BaF_2:Y), and gallium doped zinc oxide (ZnO:Ga), show ultrafast scintillation light with sub-ns decay time. While they have relative lower overall light output as compared to LYSO:Ce, their light output in the 1st ns is higher than or compatible to LYSO:Ce because of their short decay time. BaF_2 is also featured with the shortest attenuation length for 40 keV X-rays, so offers a compact sensor for GHz hard X-ray imaging.

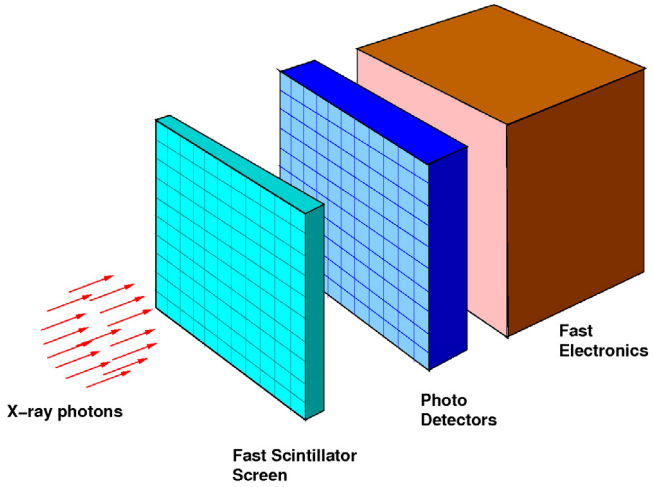

Fig. 1. A pixelated total absorption imager.

The real issues for these materials are the slow component with a 600 ns decay time for BaF_2, which would cause pileup, and the self-absorption for ZnO:Ga, which prevents its use in bulk [6]. Progresses

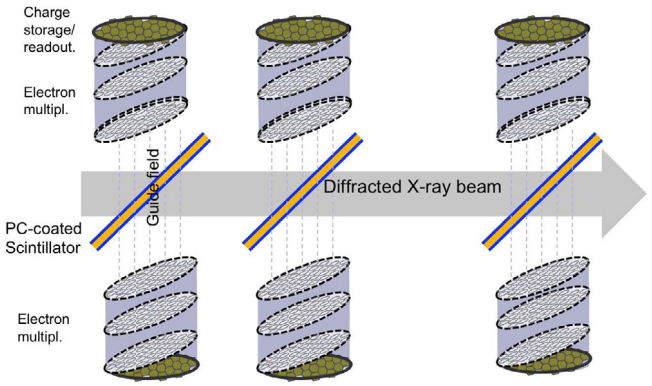

Fig. 2. A multilayer thin film imager.

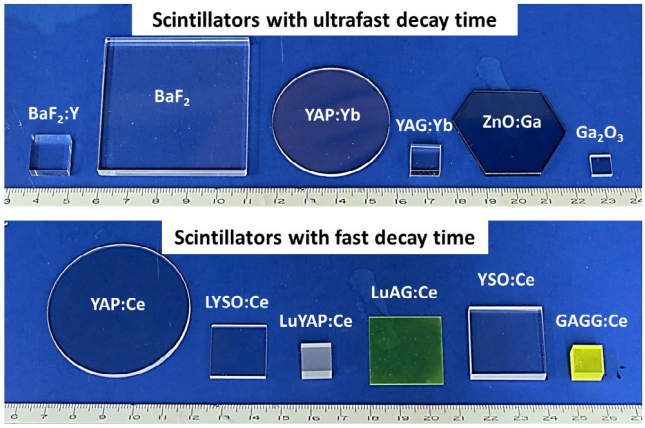

Fig. 4. Scintillators with ultrafast decay time (top) and fast decay time (bottom).

were made on these materials. Yttrium doping in BaF_2 was found to be effective in significantly improving the Fast/Slow ratio while keeping the amount of the ultrafast scintillation component unchanged [5]. ZnO:Ga nano-particle imbedded in polystyrene shows a 0.5 ns decay time [3].

We proposed two ultrafast scintillator-based front imager concepts for GHz hard X-ray imaging: a total absorption concept and a multilayer concept. Fig. 1 shows a total absorption X-ray imager, where pixelated BaF_2 crystals are coupled to a matching pixelated ultrafast photodetector and readout by fast electronics [2]. This approach is similar to an ultrafast BaF_2 crystal calorimeter being pursued by the HEP community [7]. The advantage of this concept is its high absorption efficiency for hard X-rays. With a 5 mm thick crystal screen almost 100% X-rays of up to more than 100 keV are absorbed in the crystal, maximizing dynamic range of the imaging. A limiting factor for this concept is its spatial resolution which is defined by the pixel size in the crystal screen. Fig. 2 shows the multilayer detector concept, where each layer consists of an ultrafast scintillator thin film coated with high QE photocathode layer. A magnetic field perpendicular to the X-ray direction guides the photoelectrons to amplification and storage [4]. The advantage of this concept is high spatial resolution because of the thin film thickness. The disadvantage of this concept is a low overall X-ray absorption efficiency limited by the layer number and the dead material along the X-ray path.

We tested the inorganic scintillators listed in Table 2 at the 10-ID-B site of the Advanced Photon Source (APS) of ANL. Their temporal response to the hybrid X-ray beam, including rise time, decay time and full width at half maximum (FWHM) pulse width, were measured. Their ability to resolve X-ray bunches with 2.83 ns bunch spacing were tested, which provides a proof of principle for the ultrafast inorganic scintillator-based front imager for GHz hard X-ray imaging.

2. Hybrid X-ray beam at APS, samples and measurement setup

We measured rise time, decay time and FWHM pulse width for twelve ultrafast and fast inorganic scintillators at the 10-ID-B site of APS by using hybrid X-ray beam, consisting of singlet bunches and eight septuplet bunches. Its fill pattern consists of a burst of X-rays generated by a single electron bunch and a consecutive series of electron bunches. Fig. 3 shows the characteristic of the hybrid fill pattern. The total current is 102 mA. A single bunch of 16 mA is isolated from eight septuplet bunches by symmetrical 1.594 μs gaps. The eight groups of septuplet bunches, with a maximum current of 11 mA per group, have a periodicity of 68 ns and a gap of 51 ns between groups. The bunch lengths of the singlet and the septuplet bunch are 50 and 27 ps, respectively, which have a negligible influence on the measured temporal response. Time between bunches within a septuplet bunch is 2.83 ns, which is compatible with the MaRIE Type I imager of 2 ns. Detailed information of the hybrid beam is listed on the APS online webpage [8].

Fig. 4 shows the twelve scintillators measured at APS. They are arranged on the basis of the measured FWHM pulse width. While the six ultrafast scintillators with pulse width of less than 10 ns are on

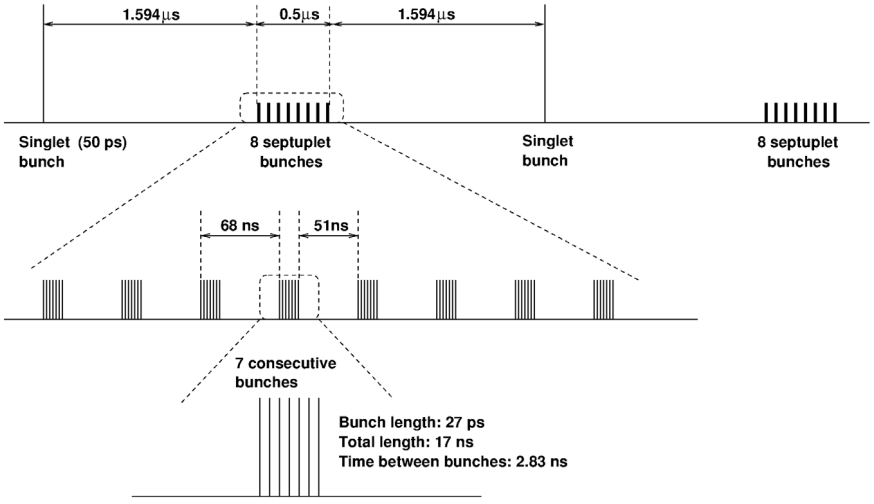

Fig. 3. A schematic showing characteristics of the hybrid beam.

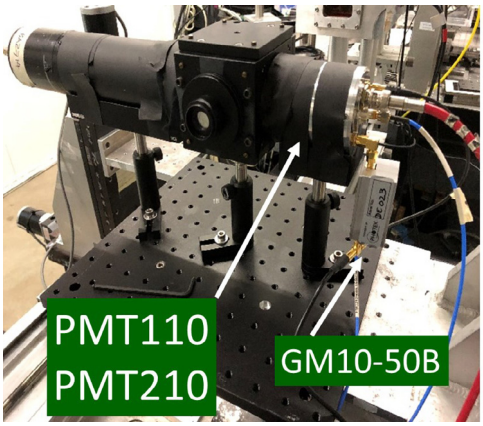

Fig. 5. A photo showing Photek PMT110/210 equipped with a gate unit GM10-50B.

the top row, the other six fast scintillators are on the bottom row. Fig. 5 is a photo showing the experimental setup on an aluminum breadboard inside the 10 ID-B irradiation room. Also shown are Photek microchannel plate PMT (MCP-PMT) 110 or 210 together with a gate unit Photek GM10-50B.

Fig. 6 shows a schematic of the APS test setup. Crystals, MCP-PMT and the gate unit were in the hutch at the APS 10-ID-B site. A Tektronix digital oscilloscope DPO 71254C (12.5 GHz, 100 GS/s), a delay generator SRS DG535 and a HV power supplier were in the control room. Signal from MCP-PMT went through a 15 m wideband SMA cable, which actually compromised the observed temporal response for ultrafast scintillators, such as BaF_2 and ZnO:Ga.

Table 3 lists technical characteristics of various photodetectors used in this investigation. All photodetectors are featured with a quartz window and a VUV sensitive cathode with 25% quantum efficiency for the ultrafast scintillation peaked at 220 nm from BaF_2 and BaF_2:Y. Both Photek MCP-PMT 110 and 210 have an ultrafast rise time of less than 100 ps and a FWHM pulse width of less than 200 ps, which are more than a factor of ten faster than the 1.3 ns and 3 ns respectively of the classical Hamamatsu R2059 PMT. The ultrafast nature of the Photek MCP-PMTs is crucial for this investigation. While the Photek MCP-PMT 110 is faster than 210, its low gain makes it difficult to measure samples with low light output in the 1st ns, such as Yb doped YAP and YAG and β-Ga_2O_3 crystals. We thus used both Photek MCP-PMT 110 and 210 in this investigation.

3. Experimental results

We present the results of this investigation in two parts: crystal's response to septuplet bunches to see its capability for 2.83 ns bunch spacing, and crystal's temporal response to singlet bunches to see its rise, decay and FWHM pulse width. Fig. 7 shows the hybrid beam measured by BaF_2:Y with Photek MCP-PMT 210. Both the singlet bunch and the eight groups of septuplet bunches are observed. The separation between these two kinds of bunches is about 1.6 μs. The total length of the eight septuplet bunch train is about 500 ns. The intensity of the singlet bunch is much higher than the septuplet bunches due to its higher fill current.

Figs. 8 and 9 show crystal's response to eight and the leading two septuplet bunches respectively for BaF_2:Y, BaF_2, ZnO:Ga, and LYSO:Ce. Clear septuplet structures with 2.83 ns bunch spacing were observed by BaF_2:Y, BaF_2, and ZnO:Ga at a less level, but not by LYSO:Ce and other crystals with long decay time. Amplitude reduction is also observed for eight septuplets in BaF_2 and LYSO:Ce, but not in BaF_2:Y and ZnO:Ga, which is due to PMT saturation caused by the slow scintillation in BaF_2 and LYSO:Ce. A smaller amplitude in BaF_2:Y than BaF_2 is observed, which is due to a mis-alignment of the small BaF_2:Y sample for the MCP-PMT 210 runs.

Fig. 10 shows BaF_2's response to a septuplet bunch, which is featured with clearly resolved X-ray bunches with 2.83 ns bunch spacing, providing a proof of principle for the ultrafast inorganic scintillator-based front imager for GHz hard X-ray imaging. Compared to BaF_2, BaF_2:Y has a similar sub-ns scintillation component and a suppressed slow component [5]. A better X-ray imaging is expected by BaF_2:Y crystals with a reduced cable length and a higher sampling rate.

Figs. 11 and 12 show temporal response to singlet bunch measured by BaF_2:Y, BaF_2, ZnO:Ga, and LYSO:Ce using a Photek MCP-PMT110, where crystals are well aligned to the beam. We note that the peak amplitudes of BaF_2 and BaF_2:Y are higher than ZnO:Ga and LYSO:Ce, which is consistent with the values of the light output in the 1st ns listed in Table 2. Compared to ZnO:Ga, the decay time of BaF_2 and BaF_2:Y are also a factor of two shorter. This indicates that BaF_2 and BaF_2:Y are better candidate scintillators for ultrafast X-ray imaging. We also noticed that the observed rise and decay time of BaF_2 and BaF_2:Y are longer than the γ -ray source data measured at Caltech crystal lab [6], which is due to the 15 m cable length as demonstrated in measurements carried out after the APS test.

Figs. 13, 14 and 15 show temporal response of all other crystals, except for BaF_2 and BaF_2:Y, using the Photek MCP-PMT 210. Compared to BaF_2 and BaF_2:Y, YAP:Yb, YAG:Yb and ZnO:Ga, show a slower response. Their FWHM width, however, is still less than 2 ns, so might work for GHz X-ray imaging. Their light output in the 1st ns, on the

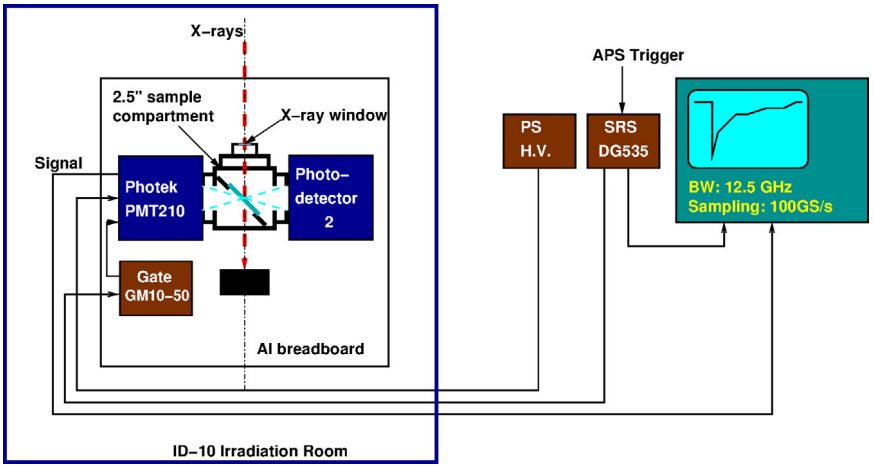

Fig. 6. A schematic showing the APS test setup.

Table 3
Technical characteristics of various UV sensitive photodetectors.

PD	Active area (mm^2)	Spectral range (nm)	Peak sensitivity (nm)	Gain	Rise time (ns)	FWHM (ns)
Hamamatsu PMT R2059	Φ46	160–650	450	2×10^7	1.3	3
Photek MCP-PMT110	Φ10	160–850	280–450	1×10^4	0.065	0.11
Photek MCP-PMT210	Φ10	160–850	280–450	1×10^6	0.095	0.17
Photek MCP-PMT240	Φ40	160–850	280–450	1×10^6	0.18	0.85

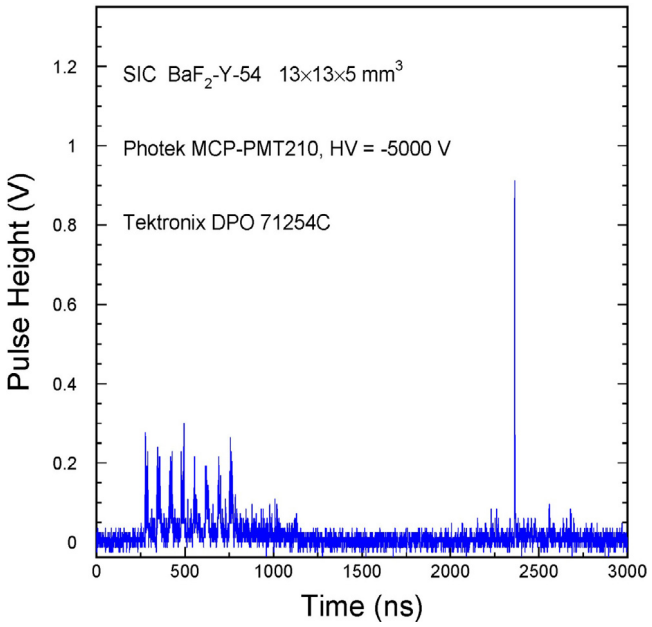

Fig. 7. Hybrid beam measured by BaF_2:Y.

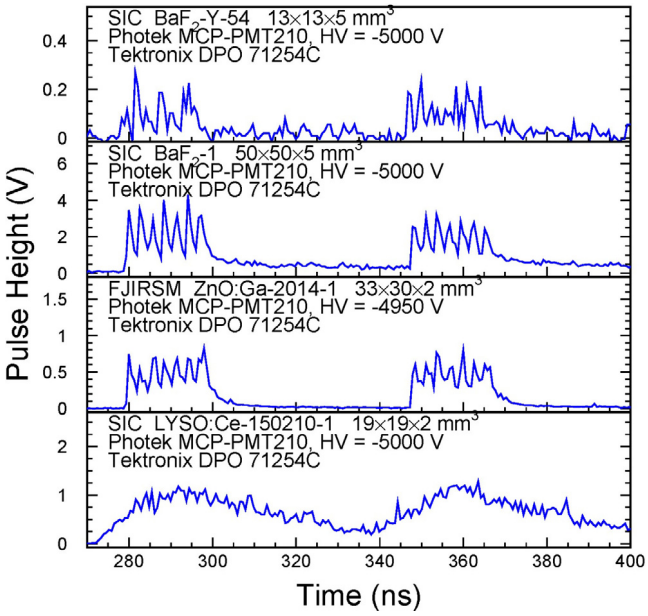

Fig. 9. Imaging for 2 septuplet bunches measured by BaF_2:Y, BaF_2, ZnO:Ga, and LYSO:Ce, respectively.

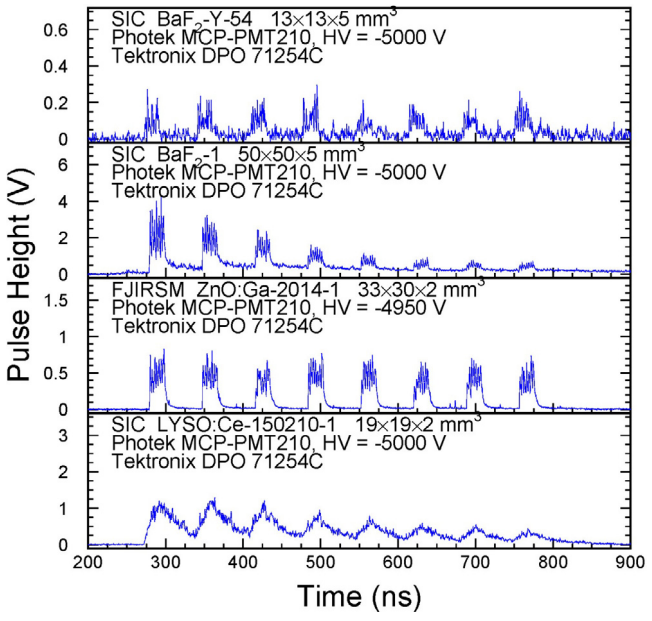

Fig. 8. Imaging for eight septuplet bunches measured by BaF_2:Y, BaF_2, ZnO:Ga, and LYSO:Ce.

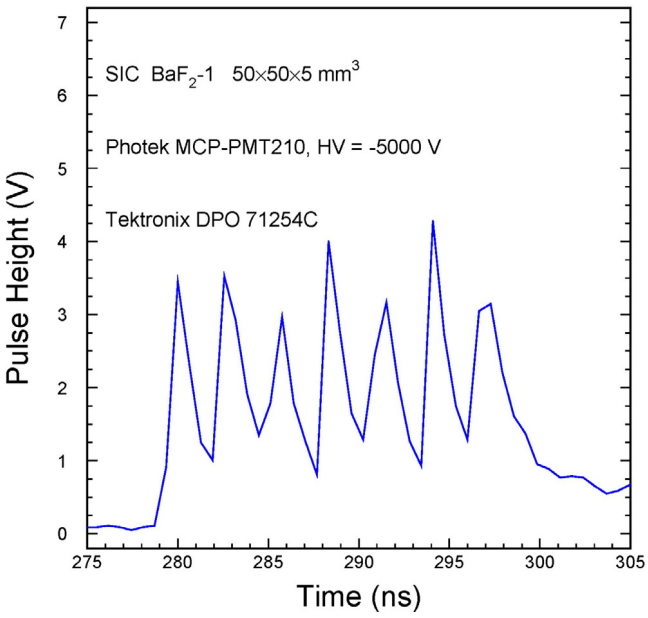

Fig. 10. BaF_2 imaging for 2.83 ns bunch spacing.

other hand, are too low to be considered seriously. Figs. 14 and 15 show decay time measured for other crystals to singlet bunches. These crystals are too slow for GHz X-ray imaging.

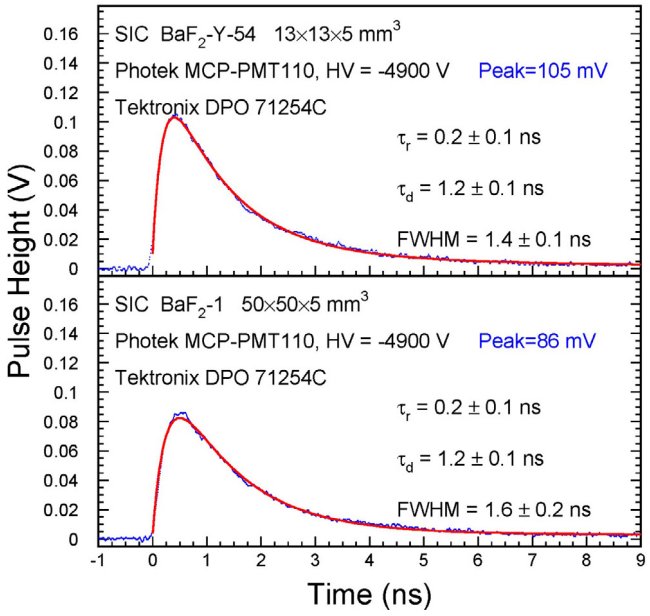

Fig. 11. Singlet bunch measured by BaF_2:Y (top) and BaF_2 (bottom) using a Photek MCP-PMT110.

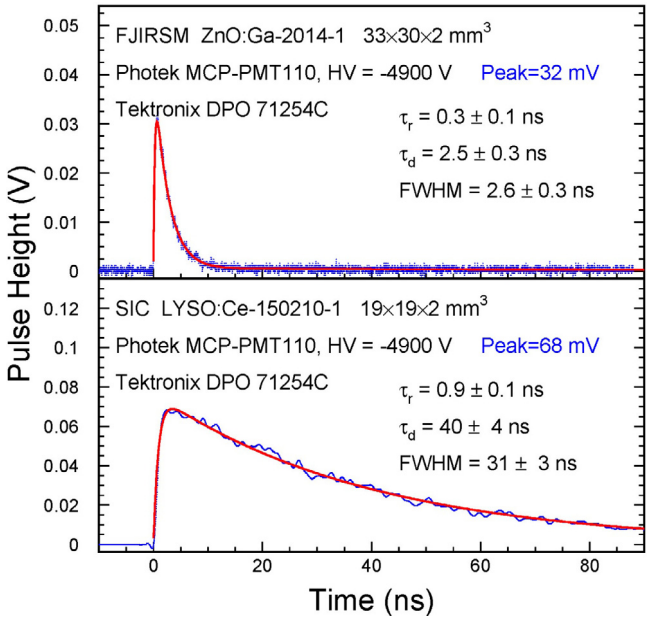

Fig. 12. Singlet bunch measured by ZnO:Ga (top) and LYSO:Ce (bottom) using a Photek MCP-PMT110.

Table 4 summarizes temporal response measured by the Photek MCP-PMT 210 for all twelve crystals investigated in this work. Samples are listed based on their FWHM values to the singlet bunch. Both BaF_2:Y and BaF_2 show the best temporal response among all these samples. We plan to concentrate on BaF_2:Y in our future investigation because of its reduced slow component.

4. Conclusion

We measured temporal response of a dozen ultrafast and fast inorganic scintillators at the APS 10-ID-B site by using hybrid X-ray beam, consisting of both singlet bunches of 50 ps and septuplet bunches of 27 ps with 2.83 ns bunch spacing. Ultrafast inorganic scintillators, such as

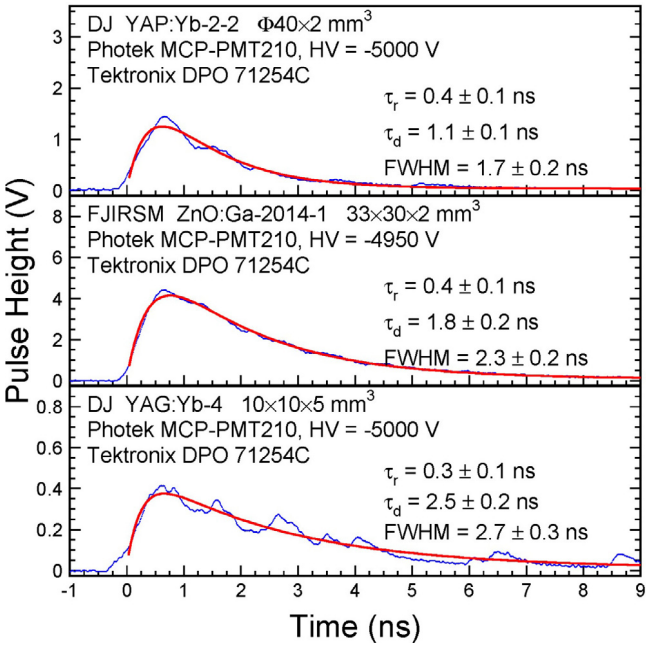

Fig. 13. Singlet bunch measured by YAP:Yb (top), ZnO:Ga (middle) and YAG:Yb (bottom) using a Photek MCP-PMT210.

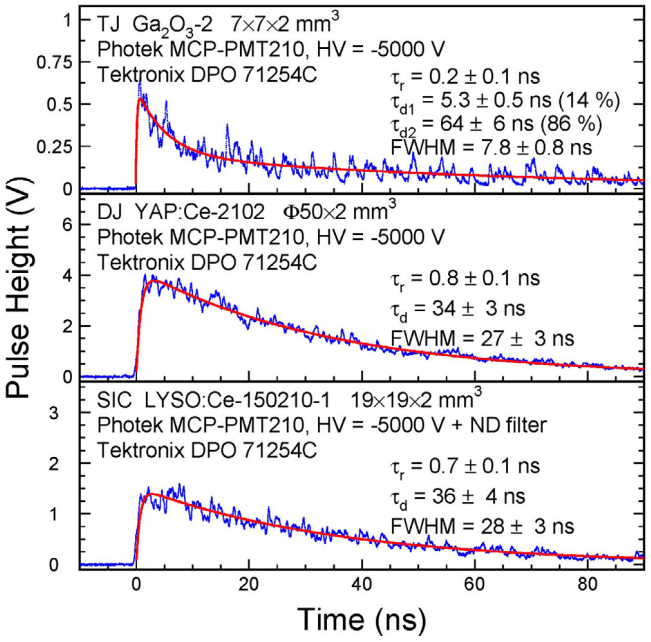

Fig. 14. Singlet bunch measured by Ga_2O_3 (top), YAP:Ce (middle) and LYSO:Ce (bottom) using a Photek MCP-PMT210.

BaF_2:Y and ZnO:Ga, show clearly resolved X-ray bunches for septuplets, as well as no degradation of amplitude for continuous eight septuplets, providing a proof of principle for the ultrafast inorganic scintillator-based total absorption front imager for the proposed MaRIE project. Other crystals are either not fast enough, such as LYSO:Ce etc., so show serious pileup effect because of their slower decay time, or not bright enough, such as Yb doped YAP and YAG crystals.

With sub-ns decay time BaF_2:Y and BaF_2 show the highest amplitude and the fastest response time among all crystals tested so far. YAP:Yb, YAG:Yb and ZnO:Ga show slower response than BaF_2. The temporal response measured for BaF_2:Y and BaF_2 at APS, however, is

Table 4
Temporal response for fast crystals scintillators.

Crystal	Vendor	ID	Dimension (mm^3)	Emission peak (nm)	EWLT (%)	LO (p.e./MeV)	LO in 1st ns (ph/MeV)	Rising time (ns)	Decay time (ns)	FWHM (ns)
BaF_2:Y	SIC	4	10 × 10 × 5	220	89.1	258	1200	0.2	1.0	1.4
BaF_2	SIC	1	50 × 50 × 5	220	85.1	209	1200	0.2	1.2	1.5
YAP:Yb	Dongjun	2-2	Φ40 × 2	350	77.7	9.1*	28	0.4	1.1	1.7
ZnO:Ga	FJIRSM	2014-1	33 × 30 × 2	380	7	76*	157	0.4	1.8	2.3
YAG:Yb	Dongjun	4	10 × 10 × 5	350	83.1	28.4*	24	0.3	2.5	2.7
Ga_2O_3	Tongji	2	7 × 7 × 2	380	73.8	259	43	0.2	5.3	7.8
YAP:Ce	Dongjun	2102	Φ50 × 2	370	54.7	1605	391	0.8	34	27
LYSO:Ce	SIC	150210-1	19 × 19 × 2	420	80.1	4841	740	0.7	36	28
LuYAP:Ce	SIPAT	1	10 × 10 × 7	385	\	1178	125	1.1	36	29
LuAG:Ce Ceramic	SIC	S2	25 × 25 × 0.4	520	52.3	1531	240	0.6	50	40
YSO:Ce	SIC	51	25 × 25 × 5	420	72.6	3906	318	2.0	84	67
GAGG:Ce	SIPAT	5	10 × 10 × 7	540	\	3212	239	0.9	125	91

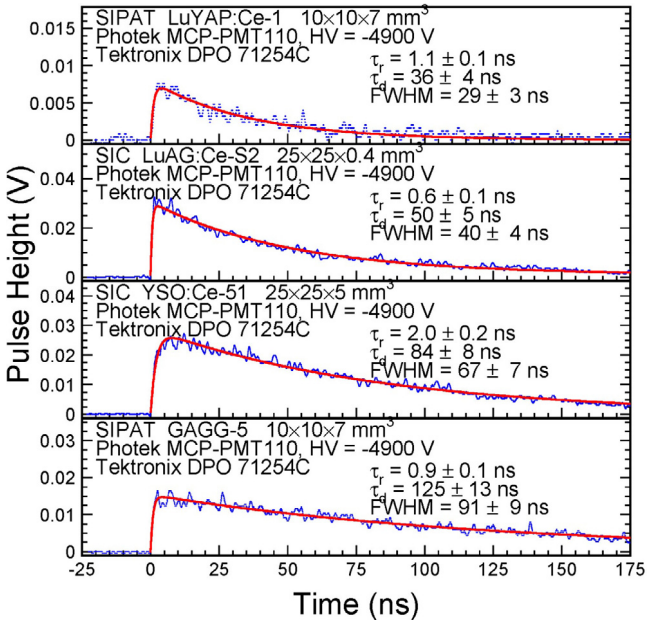

Fig. 15. Singlet bunch measured by LuYAP:Ce, LuAG:Ce ceramic, YSO:Ce and GAGG:Ce (from top to bottom) using a Photek MCP-PMT210.

slower than the data obtained with γ -ray sources at Caltech because of the 15 m long cables between the MCP-PMT and the DPO. Further development will be concentrated on BaF_2:Y crystals for the ultrafast inorganic scintillator-based front sensor with total absorption nature for GHz X-ray imaging.

Acknowledgments

This work is supported by the U.S. Department of Energy, under Award Number DE-SC0011925, DE-AC02-06CH11357 and the Los Alamos National Laboratory C2 program. The authors would also like to thank staffs at APS 10-ID-B for their beamline support. Photek provided a loan of the MCP-PMT 210 and the GM10-50B gate unit.

References

[1] C.W. Barnes, et al., Technology Risk Mitigation Research and Development for the Matter-Radiation Interactions in Extremes (MaRIE) Project, Los Alamos National Laboratory Report LA-UR-17-26474 (2017).
[2] P. Denes, S. Gruner, M. Stevens, Z. Wang (Eds.), Ultrafast and high- energy x-ray imaging technologies and applications, in: Tech. Rep. LA-UR-17-22085, Los Alamos Nat. Lab., Santa Fe, NM, USA, 2016, See imager concept by R.-Y. Zhu. Online Available: https://www.lanl.gov/science-innovation/science-facilities/marie/_assets/docs/workshops/ultrafast-high-energy-x-ray.pdf.
[3] P. Lecoq, The 10 ps Timing-of-Flight PET Challenge, in: Proc. of the SCINT 2017 Conference, Chamonix, France (2018).
[4] Z. Wang, C.W. Barnes, J.S. Kapustinsky, C.L. Morris, R.O. Nelson, F. Yang, L. Zhang, R.-Y. Zhu, Thin scintillators for ultrafast hard x-ray imaging, Proc. SPIE 9504 (2015) http://dx.doi.org/10.1117/12.2178420.
[5] R.-Y. Zhu, Applications of very fast inorganic crystal scintillators in future hep experiments, in: TIPP 2017, SPPHY 213, 2018, pp. 70–75, http://dx.doi.org/10.1007/978-981-13-1316-5_13.
[6] C. Hu, L. Zhang, R.-Y. Zhu, A. Chen, Z. Wang, L. Ying, Z. Yu, Ultrafast inorganic scintillators for gigahertz hard x-ray imaging, IEEE Trans. Nucl. Sci. 65 (2018) 2097–2104.
[7] F. Abusalma, D. Ambrose, A. Artikov, et al., Expression of Interest for Evolution of the Mu2e Experiment, Fermilab-FN-1052, arXiv:1802.02599, 2018.
[8] https://ops.aps.anl.gov/SRparameters/node5.html.